Mineralogical Magazine, October 2006, Vol. 70(5), pp. 565–578

Crystal-structure refinement of a Zn-rich kupletskite from Mont Saint-Hilaire, Quebec, with contributions to the geochemistry of zinc in peralkaline environments

P. C. Piilonen[1], I. V. Pekov[2], M. Back[3], T. Steede[3] and R. A. Gault[4]

[1] Earth Sciences Division, Canadian Museum of Nature, Ottawa, Ontario K1P 6P4, Canada
[2] Faculty of Geology, Moscow State University, Borobievy Gory, 119992 Moscow, Russia
[3] Natural History Department, Mineralogy, Royal Ontario Museum, Toronto, Ontario M5S 2C6, Canada
[4] Earth Sciences Division, Canadian Museum of Nature, Ottawa, Ontario K1P 6P4, Canada

ABSTRACT

The chemistry and crystal structure of a unique Zn-rich kupletskite: $(K_{1.55}Na_{0.21}Rb_{0.09}Sr_{0.01})_{\Sigma 1.86}(Na_{0.82}Ca_{0.18})_{\Sigma 1.00}(Mn_{4.72}Zn_{1.66}Na_{0.41}Mg_{0.12}Fe^{2+}_{0.09})_{\Sigma 7.00}(Ti_{1.85}Nb_{0.11}Hf_{0.03})_{\Sigma 1.99}(Si_{7.99}Al_{0.12})_{\Sigma 8.11}O_{26}$ $(OH)_4(F_{0.77}OH_{0.23})_{\Sigma 1.00}$, from an alkaline pegmatite at Mont Saint-Hilaire, Quebec, Canada has been determined. Zn-rich kupletskite is triclinic, $P\bar{1}$, a = 5.3765(4), b = 11.8893(11), c = 11.6997(10), α = 113.070(3), β = 94.775(2), γ = 103.089(3), $R1$ = 0.0570 for 3757 observed reflections with $F_o > 4\sigma(F_o)$. From the single-crystal X-ray diffraction refinement, it is clear that Zn^{2+} shows a preference for the smaller, *trans* $M(4)$ site (69%), yet is distributed amongst all three octahedral sites coordinated by 4 O^{2-} and 2 OH^- [$M(2)$ 58% and $M(3)$ 60%]. Of note is the lack of Zn in $M(1)$, the larger and least-distorted of the four crystallographic sites, with an asymmetric anionic arrangement of 5 O^{2-} and 1 OH^-. The preference of Zn for octahedral sites coordinated by mixed ligands (O and OH) is characteristic of its behaviour in alkaline systems, in contrast to granitic systems where Zn tends to favour [4]-coordinated, OH- and H_2O-free sites with only one ligand species (O, S, Cl, B, I). In alkaline systems, $^{[4]}Zn$ is only present in early sphalerite or in late-stage zeolite-like minerals. The bulk of Zn in alkaline systems is present as discrete $^{[6]}Zn$ phases such as members of the astrophyllite, labuntsovite, milarite and nordite groups, a result of the formation of network-forming $Zn(OH)_4^{2-}$ complexes in the low-temperature, low-f_{S_2}, high-alkalinity and highly oxidizing systems.

Keywords: zinc, ordering alkaline, astrophyllite-group, pegmatite, kupletskite.

Introduction

Kupletskite, ideally $K_2NaMn_7Ti_2Si_8O_{26}(OH)_4F$, a member of the heterophyllosilicate astrophyllite-group, was first described by Semenov (1956) from nepheline syenite pegmatites in the Lepkhe-Nelm and Kuivchorr mountains of the Lovozero massif, Kola Peninsula, Russia. Since then, it has been found in a variety of SiO_2-oversaturated and SiO_2-undersaturated alkaline intrusions including the Burpala massif, Siberia, Russia (Chukrov, 1972), Point of Rocks, New Mexico, USA (DeMark, 1984), Gjerdingen, Norway (Raade and Haug, 1982), the Junguni intrusion, Chilwa, Malawi (Woolley and Platt, 1988), Khibiny massif, Kola Peninsula, Russia (Kostyleva-Labuntsova *et al*., 1978), the Mariupol complex, Azov sea region, Ukraine (Valter *et al*., 1965), the Larvik complex, Langesundsfjord area, Norway (Piilonen *et al*., 2003*a*), the Werner Bjerge complex and Kangerdlugssuaq, East Greenland (Brooks *et al*., 1982; Christiansen *et al*., 1998), Mont Saint-Hilaire, Québec, Canada (Horváth and Gault, 1990; Piilonen *et al*., 2000, 2003*a*), Zaangarskii massif, Siberia, Russia (Sveshnikova *et al*., 1976), and the Tamazeght complex, High

* E-mail: ppiilonen@mus-nature.ca
DOI: 10.1180/0026461067050350

Atlas mountains, Morocco (Kadar, 1984). Kupletskite generally occurs as a rare primary to post-magmatic mineral in alkaline pegmatites and late-stage vugs.

During a reconnaissance examination of a suite of astrophyllite-group minerals (AGM) from the mineralogy collection at the Royal Ontario Museum (ROM), an unusual kupletskite was discovered in an alkaline pegmatite from the Poudrette Quarry, Mont Saint-Hilaire, Québec. The kupletskite in question (CP2535/M52204 and CP2536/M52205) was collected in 1985 by Ms Cynthia Peat, and later donated to the ROM. The samples were labelled 'Zn-kupletskite', and records referred to them as 'zincian' kupletskite; initial X-ray fluorescence (XRF) analyses were performed on these and other donated astrophyllite-group samples by Mr R. Ramik (ROM), confirming that indeed the kupletskites in question were Zn-rich. Further electron microprobe (EMPA) analyses indicated these samples to contain up to 10.34 wt.% ZnO (1.726 a.p.f.u. Zn), an order of magnitude more ZnO than has been noted for kupletskite, on average, in the literature to date (Table 1). Crystals are stepped, subhedral and lustrous, grading from brown to beige, with the lighter, beige zones being enriched in ZnO. Associated minerals include aegirine, analcime, catapleiite, bastnäsite, microcline, polylithionite, pyrochlore and serandite.

A closer examination of the literature available concerning Zn in alkaline rocks revealed many references alluding to substitution of Zn in Mn-Fe-Mg silicates, yet a lack of detailed discussions on the crystal-chemistry and geochemistry of Zn in alkaline igneous systems. This study examines the crystal-chemical role of Zn in the astrophyllite-group structure, and sheds light on the crystal-chemistry and behaviour of Zn in plutonic alkaline environments, in particular those of late-stage alkaline pegmatites.

Chemical composition

Chemical analyses of the Zn-rich kupletskite were performed on a JEOL 733 electron microprobe at the Canadian Museum of Nature using Tracor Northern 5500 and 5600 automation in wavelength dispersive mode. The operating conditions were as follows: beam diameter of 20 μm, operating voltage of 15 kV and a beam current of 20 nA. Data reduction was performed using a PAP routine in XMAQNT (C. Davidson, CSIRO). Overlap corrections for Si($K\alpha$)-Sr($L\alpha$), Zr($L\beta$)-Nb($L\alpha$) and Mn($K\beta$)-Nb($L\alpha$) were done. A total of 24 elements were sought and the following standards were employed: Na-amphibole (Na-$K\alpha$ and Si-$K\alpha$), sanidine (K-$K\alpha$ and Al-$K\alpha$), diopside (Ca-$K\alpha$ and Mg-$K\alpha$), tephroite (Mn-$K\alpha$), almandine (Fe-$K\alpha$), rutile (Ti-$K\alpha$), synthetic $MnNb_2O_6$ (Nb-$L\alpha$), vlasovite (Zr-$L\alpha$), zincite (Zn-$L\alpha$), phlogopite (F-$K\alpha$), pollucite (Cs-$L\alpha$), celestite (Sr-$L\alpha$), sanbornite (Ba-$L\alpha$), rubidium microcline (Rb-$L\alpha$), synthetic $NiTa_2O_6$ (Ta-$M\alpha$), and hafnon (Hf-$M\alpha$). Count times for all elements were 25 s or 0.5% precision, whichever was obtained first, except for Cs and Rb (100 s), and Hf (50 s). Also sought but not detected were La, Ce, Yb, P, Th, Pb, Ni, V, U, W, Sc, S and Mo. Complete EMPA data can be found in Table 1. The average empirical formula (average of nine analyses) is $(K_{1.55}Na_{0.21}Rb_{0.09}Sr_{0.01})_{\Sigma 1.86}$ $(Na_{0.82}Ca_{0.18})_{\Sigma 1.00}$ $(Mn_{4.72}Zn_{1.66}Na_{0.41}Mg_{0.12}Fe^{2+}_{0.09})_{\Sigma 7.00}$ $(Ti_{1.85}Nb_{0.11}Hf_{0.03})_{\Sigma 1.99}(Si_{7.99}Al_{0.12})_{\Sigma 8.11}O_{26}$ $(OH)_4(F_{0.77}OH_{0.23})_{\Sigma 1.00}$ based on 31 anions as determined during crystal structure analysis and following methods outlined by Piilonen *et al.* (2003*a*).

Infrared analysis

Fourier transform infrared (FTIR) spectroscopy was performed at the Canadian Conservation Institute using a Bomem Michelson MB120 spectrometer interfaced to a Spectra-Tech IR Plan Research microscope equipped with a 0.25 mm diameter, narrow-band MCT (mercury cadmium telluride) detector. The sample was positioned in a Spectra-Tech low-pressure diamond anvil cell and pressed into a thin film and masked with fixed 100 μm circular apertures. Spectra were acquired in the 4000 to 660 cm^{-1} range at a resolution of 4 cm^{-1}, by co-addition of 200 interferograms. The FTIR spectrum of Zn-rich kupletskite (Fig. 1) includes bands at 3639 (O–H stretching), 1652w (H–O–H bending), 1057 to 970 (Si–O stretching), and 696 cm^{-1} (Si–O bending).

X-ray crystallography

Powder X-ray diffraction data were collected for 24 h on a 114.6 mm Gandolfi camera (Cu-$K\alpha$ radiation, Ni filter) operating at 35 kV and 20 mA. The data were indexed using the unit cell obtained from the single-crystal X-ray diffraction data [a = 5.3765(4), b = 11.8893(11), c = 11.6997(10), α = 113.070(3), β = 94.775(2),

TABLE 1. EMPA analyses (wt.% oxides and atoms per formula unit) of Zn-rich kupletskite.

Sample #	2535-1	2535-2	2535-3	2535-4	2536-1	2536-2	2536-3	2536-3	2536-4	Average	Min	Max	SD
Na_2O	2.94	3.36	2.81	3.68	3.08	3.47	3.05	3.16	3.74	3.25	2.81	3.74	0.33
K_2O	5.41	5.38	5.48	5.20	5.45	5.25	5.50	5.43	5.07	5.35	5.07	5.50	0.15
Rb_2O	0.70	0.58	0.65	0.54	0.65	0.64	0.74	0.64	0.66	0.64	0.54	0.74	0.06
Cs_2O	0.00	0.00	0.00	0.00	0.00	0.00	0.00	0.00	0.00	0.00	0.00	0.00	0.00
CaO	1.07	0.90	1.05	0.17	0.96	0.53	0.93	0.99	0.18	0.75	0.17	1.07	0.36
SrO	0.07	0.08	0.03	0.05	0.04	0.03	0.05	0.06	0.04	0.05	0.03	0.08	0.02
BaO	0.00	0.00	0.00	0.00	0.00	0.00	0.00	0.00	0.00	0.00	0.00	0.00	0.00
MgO	0.36	0.38	0.36	0.32	0.35	0.37	0.33	0.38	0.31	0.35	0.31	0.38	0.03
MnO	24.12	24.05	24.79	24.74	24.41	24.71	24.52	24.44	25.62	24.60	24.05	25.62	0.46
FeO	0.46	0.56	0.61	0.44	0.49	0.41	0.48	0.50	0.44	0.49	0.41	0.61	0.06
ZnO	10.02	10.34	9.29	9.67	9.90	9.82	10.23	10.07	9.72	9.90	9.29	10.34	0.32
Al_2O_3	0.69	0.50	0.70	0.11	0.59	0.19	0.68	0.63	0.06	0.46	0.06	0.70	0.26
TiO_2	11.19	11.01	11.06	10.35	11.00	10.67	10.96	11.07	10.13	10.83	10.13	11.19	0.36
ZrO_2	0.00	0.17	0.00	0.65	0.00	0.43	0.00	0.00	0.92	0.24	0.00	0.92	0.35
HfO_2	0.00	0.00	0.00	0.00	0.00	0.00	0.00	0.00	0.00	0.00	0.00	0.00	0.00
Nb_2O_5	0.92	0.94	1.03	1.22	1.01	1.07	1.13	0.99	1.27	1.06	0.92	1.27	0.12
Ta_2O_5	0.00	0.00	0.00	0.00	0.00	0.00	0.00	0.00	0.00	0.00	0.00	0.00	0.00
SiO_2	34.76	35.23	34.80	35.96	35.18	35.65	34.62	34.97	35.88	35.23	34.62	35.96	0.50
F	0.99	0.94	1.12	1.04	0.91	1.39	1.07	1.12	1.11	1.08	0.91	1.39	0.14
H_2O	2.82	2.87	2.76	2.82	2.88	2.65	2.78	2.78	2.80	2.80	2.65	2.88	0.07
O=F	−0.42	−0.40	−0.47	−0.44	−0.38	−0.59	−0.45	−0.47	−0.47	−0.45	−0.59	−0.38	0.06
Total	96.09	96.89	96.06	96.52	96.51	96.70	96.63	96.76	97.48	96.63	96.06	97.48	0.43
Formulae based on 31 anions													
Sample #	CP2535-1	CP2535-2	CP2535-3	CP2535-4	CP2536-1	CP2536-2	CP2536-3	CP2536-3	CP2536-4	Average	Min	Max	SD
Na	0.11	0.26	0.08	0.21	0.14	0.23	0.23	0.23	0.38	0.21	0.08	0.38	0.09
K	1.57	1.55	1.59	1.50	1.58	1.52	1.60	1.57	1.46	1.55	1.46	1.60	0.05
Rb	0.10	0.08	0.10	0.08	0.10	0.09	0.11	0.09	0.10	0.09	0.08	0.11	0.01
Cs	0.00	0.00	0.00	0.00	0.00	0.00	0.00	0.00	0.00	0.00	0.00	0.00	0.00
Sr	0.01	0.01	0.00	0.01	0.01	0.00	0.01	0.01	0.01	0.01	0.00	0.01	0.00
Ba	0.00	0.00	0.00	0.00	0.00	0.00	0.00	0.00	0.00	0.00	0.00	0.00	0.00
Sum A	1.80	1.91	1.77	1.80	1.82	1.85	1.94	1.90	1.94	1.86	1.77	1.94	0.06
Na	0.74	0.78	0.74	0.96	0.77	0.87	0.77	0.76	0.96	0.82	0.74	0.96	0.09
Ca	0.26	0.22	0.26	0.04	0.23	0.13	0.23	0.24	0.04	0.18	0.04	0.26	0.09
Sum B	1.00	1.00	1.00	1.00	1.00	1.00	1.00	1.00	1.00	1.00	1.00	1.00	0.00
Na	0.45	0.43	0.42	0.45	0.45	0.42	0.35	0.40	0.30	0.41	0.30	0.45	0.05
Mg	0.12	0.13	0.12	0.11	0.12	0.13	0.11	0.13	0.11	0.12	0.11	0.13	0.01
Mn	4.66	4.61	4.78	4.74	4.69	4.74	4.73	4.69	4.89	4.72	4.61	4.89	0.08
Fe^{2+}	0.09	0.11	0.12	0.08	0.09	0.08	0.09	0.09	0.08	0.09	0.08	0.12	0.01
Zn	1.69	1.73	1.56	1.62	1.66	1.64	1.72	1.69	1.62	1.66	1.56	1.73	0.05
Sum C	7.00	7.00	7.00	7.00	7.00	7.00	7.00	7.00	7.00	7.00	7.00	7.00	0.00
Ti	1.92	1.87	1.90	1.76	1.88	1.82	1.88	1.89	1.72	1.85	1.72	1.92	0.07
Zr	0.00	0.02	0.00	0.07	0.00	0.05	0.00	0.00	0.10	0.03	0.00	0.10	0.04
Hf	0.00	0.00	0.00	0.00	0.00	0.00	0.00	0.00	0.00	0.00	0.00	0.00	0.00
Nb	0.09	0.10	0.11	0.13	0.10	0.11	0.12	0.10	0.13	0.11	0.09	0.13	0.01
Ta	0.00	0.00	0.00	0.00	0.00	0.00	0.00	0.00	0.00	0.00	0.00	0.00	0.00
Sum D	2.01	1.99	2.00	1.96	1.98	1.97	1.99	1.99	1.95	1.98	1.95	2.01	0.02
Si	7.92	7.97	7.93	8.14	7.98	8.07	7.88	7.93	8.09	7.99	7.88	8.14	0.09
Al	0.19	0.13	0.19	0.03	0.16	0.05	0.18	0.17	0.02	0.12	0.02	0.19	0.07
Sum T	8.11	8.10	8.12	8.17	8.13	8.12	8.07	8.09	8.10	8.11	8.07	8.17	0.03
F	0.72	0.67	0.81	0.74	0.65	1.00	0.77	0.80	0.79	0.77	0.65	1.00	0.10
OH	4.29	4.33	4.19	4.26	4.35	4.01	4.23	4.20	4.21	4.23	4.01	4.35	0.10
O	30.29	30.33	30.19	30.26	30.35	30.01	30.23	30.20	30.21	30.23	30.01	30.35	0.10
Σ cations	19.91	19.99	19.89	19.92	19.93	19.94	20.00	19.98	19.99	19.95	19.89	20.00	0.04
Mn#	0.98	0.98	0.98	0.98	0.98	0.98	0.98	0.98	0.98	0.98	0.98	0.98	0.00

SD: Standard deviation,
Mn# = $Mn/(Mn+Fe_{tot})$

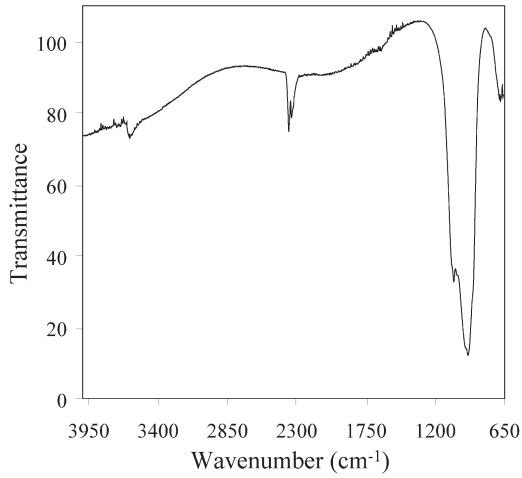

FIG. 1. FTIR spectrum of Zn-rich kupletskite.

$\gamma = 103.089(3)$] and are presented in Table 2. The measured pattern is almost identical to that observed for triclinic kupletskite from Mount Kuivchorr, Lovozero massif, Kola Peninsula, Russia (Piilonen *et al.*, 2001). The intensity data for Zn-rich kupletskite were collected using the Siemens SMART system at the University of Copenhagen (Denmark) consisting of a four-circle goniometer and a 1 K (diameter: 9 cm, 512×512 pixel) charge-coupled device (CCD) area detector. Data were collected at room temperature using monochromatic Mo-$K\alpha$ X-radiation, with the *X*-ray tube operating at 40 kV and 37 mA, a fixed detector–crystal distance of 4 cm, and a 0.5 mm collimator. A frame width (ω) of 0.2º and count exposure times of 60 s were used. Data collection consisted of 2800 frames which provided 99.5% coverage of the diffraction sphere with a mean redundancy of 2.034 times. A hemisphere of data was collected up to 71.09º2θ, with minimum and maximum indices $-8 \leqslant h \leqslant 18$, $-15 \leqslant k \leqslant 18$, and $-18 \leqslant l \leqslant 18$. Approximately 500 reflections were used to determine the orientation matrix and preliminary unit cell prior to integration of the data from all the frames. The data were reduced, filtered, integrated and corrected for Lorentz, polarization and background effects using the Siemens software SAINT. A Ψ-scan data set of 1570 reflections was chosen for absorption corrections using XPREP (Bruker Analytical X-ray Systems, 1997) with the crystal modelled as a plate on (001) with a glancing angle of 2º. The merging *R*(int) decreased from 3.70% to 3.20% after the absorption correction, giving maximum and minimum transmission-factors of 0.983 and 0.722, respectively. Phasing of a set of normalized structure factors gave a mean $|E^2-1|$ value of 1.096, suggesting the centrosymmetric space group $P\bar{1}$, consistent with other triclinic AGM (Piilonen *et al.*, 2003*b*). Information pertinent to the data collection, absorption correction and crystal structure can be found in Table 3. Structure factors (Table 4) have been deposited with the Principal Editor of the journal and are available from the Mineralogical Society's website: http://www.minersoc.org/pages/e_journals/dep_mat.html).

Results

The structure of the Zn-rich kupletskite was refined by least-squares methods using the SHELXL-93 set of programs (Sheldrick 1993), with starting parameters taken from Piilonen *et al.* (2003*b*). Refinement procedures were followed as outlined by Piilonen *et al*. (2003*b*) for other triclinic AGM. Scattering curves for neutral atoms were those of Cromer and Liberman (1970). All atom coordinates and anisotropic displacement parameters were kept as refineable parameters during the refinement process, and site occupancy factors (SOF) for all anions and Si atoms were fixed at unity. All atoms, except the split site containing K, were modelled with anisotropic thermal displacement factors. During the initial refinement, K was initially assigned to *A*, Na to *B*, Mn to the four octahedrally-coordinated sites in the *O* sheet [*M*(1) to *M*(4)], and Ti to *D*, in accordance with the dominant cations as determined by EMP analyses. Site-scattering refinements indicate the presence of a heavier X-ray scatterer in *M*(2), *M*(3) and *M*(4) (1.144, 1.134 and 0.612, respectively), as well as in *B* and *D*. Calcium and Nb were refined in *B* and *D*, respectively, with the total site occupancy constrained to be unity. Zinc was refined in *M*(2), *M*(3) and *M*(4), with each of the site occupancies constrained to be unity. No increase in *R*1 was observed, yet the total Zn content and total number of electrons as determined by the site refinement (2.322 a.p.f.u. Zn, 186 e^{-1}) were greater than that calculated from the chemical analyses (1.657 a.p.f.u. Zn, 176 e^{-1}). In order to corroborate results from the single-crystal X-ray structure refinement and chemical analyses, the site refinement of *M*(1) was modified to include a

TABLE 2. Observed and calculated powder XRD data for Zn-kupletskite.

I (%)	$d_{obs,}$ (Å)	d_{calc} (Å)	hkl	I (%)	$d_{obs,}$ (Å)	d_{calc} (Å)	hkl
100	10.610	10.5639	$00\bar{1}$	13	2.116	2.1171	$2\bar{2}3$
23	9.832	9.8015	$0\bar{1}1$			2.1144	$2\bar{3}\bar{2}$
6	5.810	5.8068	$0\bar{1}2$			2.1128	$00\bar{5}$
8	4.342	4.3343	$1\bar{2}0$			2.1127	$1\bar{4}\bar{2}$
7	4.067	4.0635	$0\bar{2}\bar{1}$	10	2.044	2.0424	$2\bar{1}3$
12	3.752	3.7484	$0\bar{2}3$	9	2.013	2.0128	132
		3.7483	$1\bar{1}2$	4	1.965	1.9663	$2\bar{5}1$
40	3.526	3.5213	$00\bar{3}$			1.9626	114
11	3.270	3.2624	$11\bar{3}$	7	1.929	1.9317	$23\bar{1}$
7	3.084	3.0791	$1\bar{2}\bar{2}$			1.9315	221
9	3.038	3.0320	$12\bar{3}$			1.9238	$0\bar{6}3$
5	2.972	2.9754	$1\bar{3}\bar{1}$	4	1.915	1.9168	$1\bar{6}1$
11	2.861	2.8640	$0\bar{1}4$			1.9114	$2\bar{5}0$
39	2.774	2.7731	$13\bar{1}$	23	1.764	1.7652	$2\bar{5}4$
		2.7717	$1\bar{4}2$			1.7633	133
33	2.650	2.6539	$11\bar{4}$			1.7624	$0\bar{6}5$
		2.6536	$2\bar{1}\bar{1}$	16	1.744	1.7448	$30\bar{1}$
46	2.573	2.5730	130			1.7432	$3\bar{2}1$
5	2.530	2.5324	$2\bar{2}\bar{1}$			1.7409	$2\bar{6}1$
21	2.489	2.4815	$2\bar{1}\bar{2}$	14	1.655	1.6570	$2\bar{2}5$
10	2.401	2.3994	$1\bar{4}\bar{1}$			1.6543	$0\bar{7}3$
		2.3989	$21\bar{2}$	9	1.631	1.6319	$2\bar{2}\bar{5}$
19	2.296	2.2962	$20\bar{3}$			1.6312	$22\bar{6}$
		2.2943	131			1.6286	$3\bar{2}\bar{3}$
11	2.235	2.2368	$1\bar{5}3$	14	1.577		
		2.2322	$2\bar{1}\bar{3}$	10	1.556		
6	2.152	2.1539	202	8	1.442		
		2.1518	$2\bar{4}2$	9	1.406		
		2.1501	$1\bar{3}\bar{3}$				
		2.1484	$0\bar{4}5$				

114.6 mm Gandolfi camera Cu-$K\alpha$ (Ni filtered) radiation. Film was scanned using an optical scanner calibrated for intensity and peak position using an external silicon standard. Indexing based on the refined structure unit cell.

fixed 0.407 a.p.f.u. Na (Table 5). No significant increase in $R1$ [0.0570 for 3757 observed reflections with $F_o > 4\sigma(F_o)$] was observed, but the Zn and Mn contents and the total number of electrons determined from the site refinements agree with those calculated from the EMPA data: 4.535 a.p.f.u. Mn, 2.058 a.p.f.u. Zn (+Fe,Mg), 0.407 a.p.f.u. Na, 180 e^{-1} from the SREF *vs.* 4.725 a.p.f.u. Mn, 1.869 a.p.f.u. Zn (+Fe,Mg), 0.407 a.p.f.u. Na, 176 e^{-1} from the chemical composition (Table 6). The slight discrepancy in Zn contents is the result of small amounts of both Fe and Mg in the chemical analyses which cannot be accounted for in the crystal-structure refinement. It is evident that the SREF and EMPA data for the *O* sheet cations agree, thus allowing us to make inferences on the ordering of Zn within the astrophyllite-group structure. Table 7 lists selected bond lengths for Zn-rich kupletskite.

Astrophyllite-group mineral nomenclature and effects of Zn substitution

The AGM structure can be considered as two composite sheets stacked along [001] in a 2:1 ratio. The first is a sheet of octahedra (*O* sheet) extending from $z \approx 0.40$ to 0.60 in triclinic species and from $z \approx -0.05$ to 0.05 in monoclinic kupletskite, which consists of a closest-packed sheet of MO_6 octahedra (where M = Mn, Fe^{2+}, Fe^{3+}, Mg or Na). There are four crystallographically distinct sites, designated $M(1)$ to $M(4)$. The

TABLE 3. Crystal structure data for Zn-rich kupletskite.

Space Group	$P\bar{1}$	Diffractometer	SIEMENS CCD
a (Å)	5.3765(4)	Radiation	Mo-$K\alpha$ (40 kV, 37 mA)
b	11.8893(11)	Crystal shape	Plate
c	11.6997(10)	Crystal size	$0.342 \times 0.198 \times$ 0.009 mm
α (°)	113.070(3)	μ (Mo-$K\alpha$)	5.69 cm^{-1}
β	94.775(2)	Min/Max trans.	0.722/0.722
γ	103.089(3)	$\lvert E^2-1\rvert$	1.096
V (Å^3)	657.7(2)	CFOM	2.39
Z	1	Glancing angle	2°

Chemical formula	$K_2Na(Mn,Zn)_7(Ti,Nb)_2Si_8O_{26}(OH)_4F$
Min/Max indices	$-8 \leqslant h \leqslant 8$, $-15 \leqslant k \leqslant 18$, $-18 \leqslant l \leqslant 18$
No. of unique reflections	5012
No. of observed reflections	3757
Criterion for observed reflections	$F_o > 4\sigma(F_o)$
R_{int}	0.0372
GooF	1.071
Final $R1$	0.0570
wR^2 (%)	0.1549

$R1 = \Sigma(|F_o|-|F_c|)/\Sigma|F_o|$

$wR^2 = \Sigma[w(F_o^2 - F_c^2)^2]/\Sigma[w(F_o^2)^2]^{1/2}$, $w = 1/\sigma^2(F_o)$

O sheet is sandwiched between two *H* sheets, extending from $Z \approx -0.15$ to -0.05. The *H* sheets consist of open-branched *zweier* [100] single chains of $[Si_4O_{12}]^{8-}$ (Liebau, 1985) which are in turn cross-linked by corner-sharing $D\phi_6$ octahedra [ϕ = unspecified anion], or DO_5 polyhedra as in magnesium astrophyllite (Shi *et al*., 1998), where D = Nb,Ti,Zr. The resultant Si:D ratio is 4:1. Individual $D\phi_6$ octahedra are linked across the interlayer space *via* $\phi(16)$. The interlayer space contains two crystallographically distinct cation sites, *A* and *B*, which are host to [11] to [13]-coordinated K and Na and [10]-coordinated Na, respectively. The general formula proposed for any AGM is:

$$A_2BC_7D_2T_8O_{26}(OH)_4X_{0-1} \quad (1)$$

where $^{[10]-[13]}A$ = K, Na, Rb, Cs, H_2O and □; $^{[10]}B$ = Na or Ca; $^{[6]}C$ = Mn, Fe^{2+}, Fe^{3+}, Na, Mg or Zn; $^{[5]-[6]}D$ = Ti, Nb, or Zr; $^{[4]}T$ = Si and Al; and $X = \phi$ = F, OH, O or □. Calculation of general formulae should be based on a total of 31 anions with 26 O and 5(OH,F,O,□). For magnesium astrophyllite, which has a vacant X site, the

TABLE 5. Refined site populations (SREF, a.p.f.u.), site scattering (e.p.f.u.) and EMPA (a.p.f.u.) values for Zn-rich kupletskite.

		Site populations (SREF)			
Site	<*M*–O>	Na	Mn	Zn	e.p.f.u.
M(1)	2.194(3)	0.2035	0.7965	0.00	44.7(1)
M(2)	2.171(3)	0.00	0.629	0.371	53.7(1)
M(3)	2.165(3)	0.00	0.659	0.341	53.4(2)
M(4)	2.129(3)	0.00	0.183	0.317	28.2(1)
	ΣSREF (a.p.f.u.)	0.407	4.535	2.058	179.9(1)
	ΣEMPA (a.p.f.u.)	0.407	4.725	1.869*	176.1(1)

* Σ = Zn+Mg+Fe

TABLE 6. Empirical bond-valences (v.u.) for Zn-rich kupletskite.

	M(1)	*M*(2)	*M*(3)	*M*(4)	*D*	*T*(1)	*T*(2)	*T*(3)	*T*(4)	*B*	*K*(1)	*K*(2)	ΣV_a
O(1)	0.31		0.38	$0.34^{X2}\downarrow$		1.01							2.04
O(2)	0.36	0.27	0.28		1.04								1.95
O(3)	0.33		0.36	$0.31^{X2}\downarrow$			1.04						2.04
O(4)			0.68	$0.40^{X2}\downarrow$									1.08
O(5)	0.34	0.74											1.08
O(6)	0.36	0.31	0.34					1.01					2.02
O(7)	0.33	0.69							0.97				1.99
O(8)							0.94	0.96			0.02		1.92
O(9)					0.70				1.08	$0.14^{X2}\downarrow$	0.13	0.04	2.09
O(10)							0.98	0.93			0.02		1.93
O(11)					0.70	1.07				$0.13^{X2}\downarrow$	0.13	0.04	2.07
O(12)					0.71				1.08	$0.13^{X2}\downarrow$	0.13	0.04	2.09
O(13)						0.96	1.04				0.08		2.08
O(14)								1.05	0.96		0.06		2.07
O(15)					0.68	1.09				$0.14^{X2}\downarrow$	0.13	0.05	2.09
ϕ(16)					$0.49^{X2}\rightarrow$					$0.08^{X2}\downarrow$	$0.07^{X2}\rightarrow$	$0.07^{X2}\rightarrow$	1.42
ΣV_c	2.03	2.01	2.04	2.10	4.32	4.13	4.00	3.95	4.09	1.24	0.75	0.25	

* constants from Brese and O'Keefe (1991)
Valences for *B*, *M* and *D* sites were calculated using the following weighted averages: B: $(Na_{0.34}Ca_{0.16})$, *M*1: $(Mn_{0.7965}Na_{0.2035})$, *M*2: $(Mn_{0.629}Zn_{0.371})$, *M*3: $(Mn_{0.659}Zn_{0.341})$, *M*4: $(Mn_{0.183}Zn_{0.317})$, *D*: $(Ti_{0.939}Nb_{0.061})$

formula should be based on 30 anions with $O_{26}(OH,F)_4$. The group has been subdivided, based on the cation dominant in the *O* sheet, into the kupletskite subgroup (Mn), the astrophyllite subgroup (Fe), and the high-alkali subgroup (Na and Mg). The subgroups can be further classified on the basis of their *D* cation composition (Ti, Nb or Zr) leading to species such as niobokupletskite and zircophyllite (Piilonen *et al.*, 2003*a*). The ideal formula for Zn-rich kupletskite is $K_2Na(Mn,Zn)_7Ti_2Si_8O_{26}(OH)_4F$.

As has been shown by Piilonen *et al.* (2003*a*,*b*), cations in the *O* sheet (Fe, Mn, Mg, Na, Zn) undergo significant ordering as a direct result of the size differences between the sites with *M*(1)>*M*(2,3)>*M*(4). In particular, Na and Mn are always strongly partitioned into the large, undistorted *M*(1) site, whereas smaller cations such as Mg and Zn show preference for the small, distorted *M*(4) site. As with other mineral groups (e.g. amphibole, eudialyte, labuntsovite, etc.), it is theoretically possible to further divide the AGM subgroups on the basis of the composition and cation ordering of the four *M* sites in the *O* sheet. If this was done, the structural and chemical formula of the group would be expressed as:

$$A_2B[M(1)_2M(2,3)_4M(4)]_7D_2T_8O_{26}(OH)_4X_{0-1} \quad (2)$$

In octahedral coordination, the divalent Zn cation, $^{[6]}Zn^{2+}$, has a similar ionic radius (0.74 Å) to that of the dominant octahedrally-coordinated divalent cations in the astrophyllite-group structure: Fe^{2+} (0.78 Å), Mn^{2+} (0.83 Å) and Mg^{2+} (0.72 Å); incorporation of Zn^{2+} into the astrophyllite-group structure *via* the substitutions $Zn^{2+} \rightleftharpoons Mn^{2+}$ or $Zn^{2+} \rightleftharpoons Fe^{2+}$ is to be expected. From the single-crystal X-ray structure refinement data, it is clear that Zn shows a preference for the smaller, *trans* *M*(4) site (69%), yet is distributed amongst all three octahedral sites coordinated by 4 O^{2-} and 2 OH^- [*M*(2) 58% and *M*(3) 60%]. Of note is the lack of Zn in *M*(1), the larger and least-distorted of the four crystallographic sites, with an asymmetric anionic arrangement of 5 O^{2-} and 1 OH^-. The distribution of Zn between *M*(2) and *M*(3) is essentially equal, with ~60% of each site occupied by Mn and 40% by Zn (Fig. 2). If we were to proceed with splitting the astrophyllite-group into species based on the dominant cation in each of the *M* sites, rather than the dominant cation in all of the *O* sheet, the number of possible species is essentially endless. Although it is of geochemical interest that Zn is dominant in the *M*(4) site and occupies almost half of two additional sites, we do not believe that a further splitting of the astrophyllite-group on the basis of

TABLE 7. Selected interatomic distances (Å) for Zn-rich kupletskite.

M(1)−O(6)	2.173(3)	*T*(1)−O(15)	1.592(4)
M(1)−O(2)	2.175(3)	*T*(1)−O(11)	1.600(4)
M(1)−OH(5)	2.187(3)	*T*(1)−O(1)	1.622(3)
M(1)−O(3)	2.198(3)	*T*(1)−O(13)	1.640(4)
M(1)−O(7)	2.205(3)	<*T*(1)−O>	1.613
M(1)−O(1)	2.228(3)		
<*M*(1)−O>	2.194	*T*(2)−O(13)	1.608(4)
		T(2)−O(3)	1.608(3)
M(2)−O(7)	2.111(3)	*T*(2)−O(10)	1.633(4)
M(2)−OH(5)	2.116(3)	*T*(2)−O(8)	1.647(4)
M(2)−OH(5)	2.136(4)	<*T*(2)−O>	1.624
M(2)−O(6)	2.200(4)		
M(2)−O(7)	2.211(3)	*T*(3)−O(14)	1.607(4)
M(2)−O(2)	2.250(3)	*T*(3)−O(6)	1.622(3)
<M2−O>	2.171	*T*(3)−O(8)	1.638(4)
		T(3)−O(10)	1.650(3)
M(3)−O(1)	2.125(3)	<*T*(3)−O>	1.629
M(3)−OH(4)	2.130(3)		
M(3)−O(3)	2.141(3)	*T*(4)−O(9)	1.595(4)
M(3)−O(6)	2.161(3)	*T*(4)−O(12)	1.595(4)
M(3)−OH(4)	2.193(4)	*T*(4)−O(7)	1.634(3)
M(3)−O(2)	2.240(3)	*T*(4)−O(14)	1.638(4)
<M(3)−O>	2.165	<*T*(4)−O>	1.615
M(4)−OH(4)	2.076(3) × 2	*K*(1)−O(11)	2.841(5)
M(4)−O(1)	2.141(3) × 2	*K*(1)−O(15)	2.843(5)
M(4)−O(3)	2.1169(3) × 2	*K*(1)−O(12)	2.844(5)
<*M*(4)−O>	2.142	*K*(1)−O(9)	2.856(5)
		K(1)−ϕ(16)	3.092(2)
D−O(2)	1.805(3)	*K*(1)−O(14)	3.384(5)
D−O(12)	1.947(4)	*K*(1)−O(14)	3.420(5)
D−O(11)	1.955(4)	*K*(1)−O(13)	3.426(5)
D−O(9)	1.955(4)	*K*(1)−O(13)	3.428(5)
D−O(15)	1.964(4)	*K*(1)−O(8)	3.595(5)
D−ϕ(16)	2.086(1)	*K*(1)−O(10)	3.667(5)
<*D*−ϕ>	1.952	*K*(1)−O(10)	3.689(5)
		<*K*(1)−O>	3.257
B−O(9)	2.590(5) × 2		
B−O(15)	2.598(5) × 2	*K*(2)−ϕ(16)	2.223(19)
B−O(12)	2.607(5) × 2	*K*(2)−O(14)	2.391(18)
B−O(11)	2.614(5) × 2	*K*(2)−O(13)	2.403(17)
B−ϕ(16)	2.688(0) × 2	*K*(2)−O(10)	2.434(18)
<*B*−ϕ>	2.619	*K*(2)−O(8)	2.439(18)
		<*K*(2)−O>	2.378

O sheet *M* site composition would be useful, or advisable, and thus we recognize a Zn-rich kupletskite and not a separate species.

Zn in alkaline systems

Although the crustal abundance of the Zn is less than that of Fe_{tot} or Mn (80 ppm *vs*. 7.00 wt.% and 1400 ppm, respectively; Faure, 1991), Zn is a relatively common element in a variety of geological environments [rock type (average ppm)]: andesite/diorite (76), basalt/gabbro (118), limestone (20) pelagic clays (165), rhyolite/rhyodacite/pantellerite (98), sandstone (16), shale (95), and ultramafic rocks (40); (values from Wedepohl 1969, Faure, 1991). However, with the exception of economically-viable Pb-Zn or Mn-Zn deposits, relatively little is known about

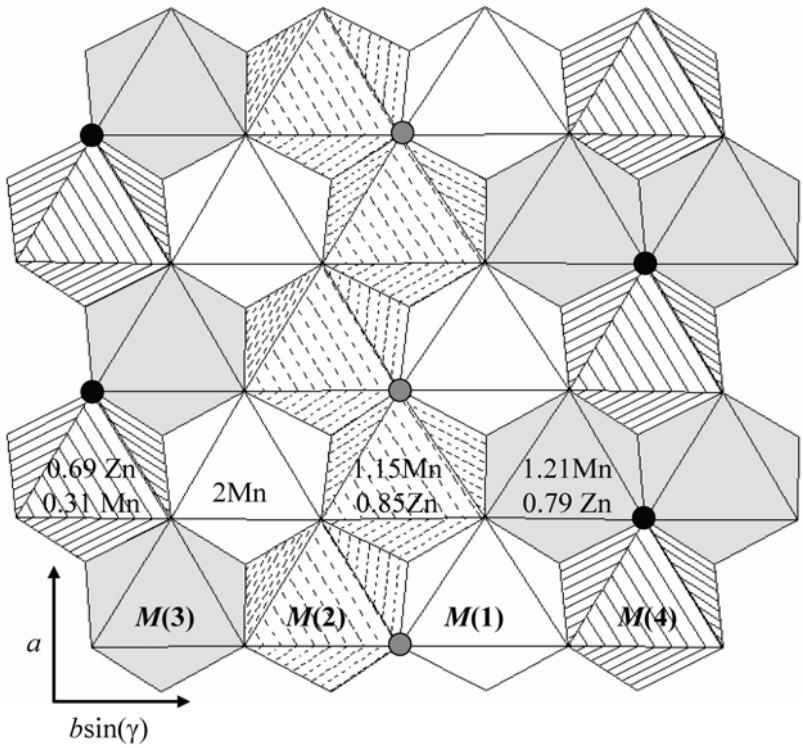

FIG. 2. Distribution of Mn and Zn between the four *M* sites in the *O* sheet of Zn-rich kupletskite. Zn shows a strong preference for the *M*(4) site, and is equally distributed between *M*(2) and *M*(3).

the crystal-chemistry and geochemistry of Zn. Although whole-rock analyses of alkaline rocks which include Zn are comparatively rare in the literature, it is clear from Fig. 3 [compilation of 278 individual and average ($N = 5-90$) analyses] that alkaline complexes and their associated pegmatites and hydrothermal phases are enriched in Zn (range: 14–3159 ppm, average: 203 ppm) relative to the bulk crust (80 ppm), and to their granitic counterparts (range: 5–235 ppm, average: 58).

To date, 172 Zn minerals have been described, 22% of which are silicates. In compounds with only one type of ligand, including oxides (e.g. franklinite, zincite, gahnite), sulphides (e.g. sphalerite, wurtzite), chlorides, bromides, iodides and some hydroxyl-free silicates (e.g. genthelvite, willemite), Zn favours tetrahedral rather than octahedral coordination ($^{[4]}Zn^{2+}$: 0.60). In these compounds, Zn displays crystal-chemical tendencies more akin to smaller [4]-coordinated cations such as Si, Al, Be, Li and Fe^{3+}, as well as other divalent cations with a similar ionic radius (Mg, Fe^{2+}, Co and Ni). This behaviour is a result of its filled *d* orbitals, high polarizability, chalcophilicity, lack of a crystal-field stabilization, and a tendency towards highly covalent, hybridized sp^3 bonds. As a result, these $^{[4]}$Zn compounds are generally OH- and H_2O-free, with dense structures containing predominantly edge- and face-shared coordination polyhedra. With the exception of alkaline environments, Zn appears to discriminate against [6]-coordinated sites in Fe-Mg silicates and forms discrete silicate minerals such as willemite and hemimorphite with Zn in [4]-coordinated sites. For example, in granitic pegmatite environments, Zn is dominantly found as sphalerite and gahnite; [6]-coordinated Zn is only present as a trace element substituting in other accessory minerals. Of note is that members of the helvite group [genthelvite/helvite, $(Mn,Zn)_4(BeSiO_4)_3S$] occur only rarely in granites which display more alkaline tendencies. In contrast, Zn behaves as a lithophile element in alkaline complexes, substituting for Mn^{2+}, Fe^{2+}, Fe^{3+} and Al^{3+} in [6]-coordinated crystallographic sites. In general, complete isomorphism between $^{[6]}$Zn and $^{[6]}Fe^{2+}$

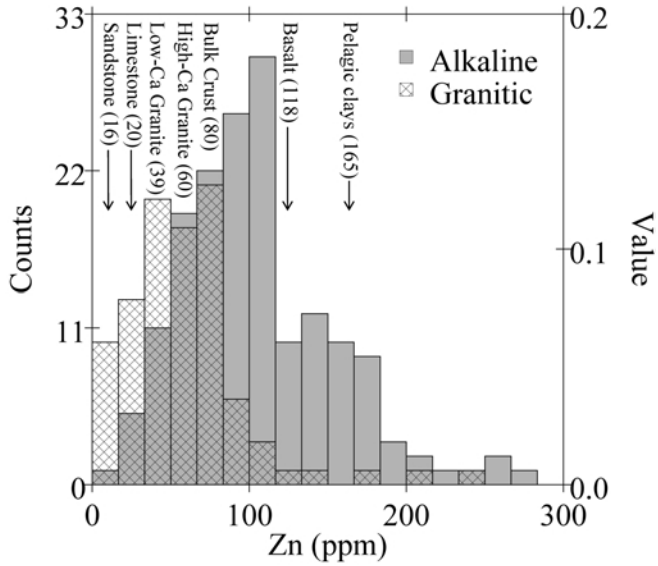

FIG. 3. Distribution of Zn (ppm) in alkaline (solid) and granitic (hatched) igneous rocks. Average Zn contents in various rock types and the bulk crust have been noted. Data compiled from Wedepohl (1969), Kovalenko (1977), Bailey *et al*. (2001), Flohr and Ross (1990), Markl (2001), Eby (2004), Eby *et al.* (1998), Peterson and Sørensen (1997), Eby (unpublished data), and Pekov (unpublished data).

or $^{[6]}$Mn is observed. In silicates containing several anion ligand species (e.g. O^{2-} and OH^{-}), Zn tends to show a preference for sites coordinated by four O^{2-} and two OH^{-} (AGM, fraiponite, hendricksite, labuntsovite-group minerals, and sauconite). Early crystallizing rock-forming minerals contain only trace concentrations of Zn: amphiboles (0.02–0.06 wt.%), pyroxenes (0.02 wt.%), and eudialyte-group minerals (0.02 wt.%; Pekov, 2002). Most Zn in alkaline systems is concentrated into late-stage peralkaline pegmatites and metasomatic/hydrothermal assemblages as discrete Zn species including sphalerite and members of the chlorite, helvite, kaolinite-serpentine, labuntsovite, milarite, nordite, phenakite, smectite, vinogradovite-lintisite and zeolite groups (for details, see Pekov, 2005). In addition to discrete Zn species, members of the following groups and series, including those of the astrophyllite group (astrophyllite, cesium kupletskite and kupletskite), have significant Zn contents (>0.5 wt.% Zn): the hilairite group (calciohilairite: up to 0.6 wt.% ZnO), the palygorskite–sepiolite family (yofortierite: up to 0.6%, sepiolite: up to 1.3%), the umbozerite series (Zn-umbozerite: up to 3.3%), the neptunite series (mangan-neptunite: up to 1.3%), and the ilmenite group (pyrophanite: up to 0.9%; Pekov, 2005). In total, 27 discrete Zn species (18 silicates, three oxides, three sulphides, two carbonate and native zinc; Table 8) have been described from such complexes, 11 of which have peralkaline pegmatites as their type localities, nine of which have been described from Mont Saint-Hilaire alone. Of these 27 species, both [4]- and [6]-coordinated Zn is observed, indicating a change in the crystal-chemical behaviour of the Zn^{2+} cation during crystallization of the various environments.

The evolution of Zn-bearing minerals in alkaline environments is not well understood. The mineralogy and behaviour of Zn in alkaline environments varies from that of a network former to a network modifier throughout a massif's evolution in response to temperature, H_2O and volatile activity, $f_{S^{2-}}$ and $f_{O^{2-}}$. As such, the speciation of Zn into various minerals can act as a petrogenetic indicator in these rocks and their derivatives. In general, early, high-temperature (450ºC), H_2O-undersaturated, high $f_{S^{2-}}$ alkaline assemblages at localities such as Mont Saint-Hilaire (Quebec) and Lovozero and Khibiny (Kola peninsula, Russia) dominantly contain minerals with network-forming [4]-coordinated Zn, with sphalerite the most important Zn species at these early stages. Other early-stage Zn minerals include wurtzite (in systems with lower $f_{S^{2-}}$), willemite, genthelvite, murataite, landauite

TABLE 8. Crystal chemistry and distribution of Zn mineral species in alkaline igneous rocks.

Mineral	Group	Formula	Zn CN	Ligands	<Zn-ϕ>	Substitutions	Environment	Early	Late	Ref
Silicates										
Zn-rich kupletskite	Astrophyllite	$K_2Na(Mn,Zn)_7Ti_2Si_8O_{26}(OH)_4F$	6	4O, 2OH	2.129	Mn, Fe	PEG		X	
Alsakharovite-(Zn)	Labuntsovite	$NaSrKZn(Ti,Nb)_4(Si_4O_{12})_2(O,OH)_4{\cdot}7H_2O$	6	4O, $2H_2O$	2.14	Mn	PEG		X	1
Baileychlore	Chlorite	$(Zn,Fe^{2+},Al,Mg)6(Si,Al)4O10(OH)8$	6	4O, 2OH		Fe^{2+}, Al, Mg	APEG		X	2
Darapiosite	Milarite	$(Na,K,\square)_3(Li,Zn,Fe)_3(Mn,Zr,Y)_2Si_{12}O_{30}$	4	4O	1.976	Li, Fe^{2+}				3
Dusmatovite	Milarite	$K(K,Na,\sim)Mn_2(Zn,Li)_3Si_{12}O_{30}$	4	4O	1.971	Li		X		3
Fraipontite	Serpentine	$(Zn,Al)_3(Si,Al)_2O_5(OH)_4$	6	2O, 4OH		Al	APEG			4
Gaultite	Lovdarite-Gaultite	$Na_4[Zn_2Si_7O_{18}]{\cdot}5H_2O$	4	4O	1.953	none	SSX		X	5
Genthelvite	Helvite	$Zn_8Si_6Be_6O_{24}S_2$	4	4O		Mn, Fe^{2+}	PEG, APEG	X		6
Hemimorphite	Hemimorphite	$Zn_4Si_2O_7(OH)_2{\cdot}H_2O$	4	4O	1.954	none	APEG		X	7
Kukisvumite	Vinogradovite	$Na_6ZnTi_4(Si_2O_6)_4O4{\cdot}4H_2O$	4	4O	2.154	none	PEG		X	8
Kuzmenkoite-(Zn)	Labuntsovite	$K_2Zn(Ti,Nb)_4(Si_4O_{12})_2(O,OH)_4{\cdot}6-8H_2O$	6	4O, $2H_2O$		Mn	PEG		X	9
Lepkhenelmite-(Zn)	Labuntsovite	$Ba_2Zn(Ti,Nb)_4(Si_4O_{12})_2(O,OH)_4{\cdot}7H_2O$	6	4O, $2H_2O$	2.10	Mn	PEG		X	10
Nordite-(Ce)	Nordite	$Na_3SrCe(Zn,Fe)Si_6O_{17}$	4	4O		Mn, Fe^{2+}, Mg	PEG, SS, SSX	X		11
Nordite-(La)	Nordite	$Na_3SrLa(Zn,Fe)Si_6O_{17}$	4	4O	1.92	Fe^{2+}, Mn, Mg	PEG, SS	X		12
Organovaite-(Zn)	Labuntsovite	$K_2Zn(Nb,Ti)_4(Si_4O_{12})_2(O,OH)_4{\cdot}6H_2O$	6	4O, $2H_2O$	2.28	Mn	PEG		X	13
Sauconite	Smectite	$Na_{0.3}Zn_3(Si,Al)_4O_{10}(OH)_2{\cdot}4H_2O$	6	4O, 2OH		Al			X	4
Shibkovite	Milarite	$K(Ca,Mn)_2(K_{2-x}\square_x)_2Zn_3Si_{12}O_{30}$	4	4O	1.959	none		X		14
Willemite	Phenakite	$ZnSi_2O_4$	4	4O	1.92	none	PEG		X	15
Zincsilite	Smectite	$Zn_3Si_4O_{10}(OH)_2{\cdot}nH_2O$	6	4O, 2OH		Mg, Mn		X		
Non-silicates										
Hydrozincite		$Zn_5(CO_3)_2(OH)_6$	4	1O,3OH			APEG		X	15
			6	2O, 4OH						
Franklinite	Spinel	$ZnFe_2^{3+}O_4$	4	4O				X	X	4
Landauite	Crichtonite	$Na[MnZn_2(Ti,Fe)_6Ti_{12}]O_{38}$	4	4O	1.964					16
Murataite		$(Y,Na)_6(Zn,Fe^{3+})_5(Ti,Nb)_{12}(O,\square)_{29}(O,F)_{10}F4$	5	5O	2.04	Fe^{3+}, Ti				17
			4	4O	1.977	Si				
Smithsonite	Calcite	$ZnCO_3$	6	6O	2.11	Mn, Fe^{2+}	APEG ?		X	4
Wurtzite-4H	Wurtzite	ZnS	4	4S	2.36			X	X	4
Wurtzite-8H	Wurtzite	ZnS	4	4S	2.36				X	4
Zinc		Zn	6	6Zn						4
Sphalerite		ZnS	4	4S	2.35			X	X	4

References: 1 - Pekov *et al*. 2003, 2 - Rule and Radke, 1988, 3 - Ferraris *et al*., 1999, 4 - Wedepohl, 1969, 5 - Ercit and van Velthuisen, 1994, 6 - Hassan and Grundy, 1985, 7 - McDonald and Cruikshank, 1967, 8 - Merlino *et al*., 2000, 9 - Chukanov *et al*., 2002, 10 - Pekov *et al*., 2004, 11 - Pekov *et al*., 1998, 12 - Pekov *et al*., 2001, 13 - Pekov *et al*., 2002, 14 - Sokolova *et al*., 1999, 15 - Ghose, 1964, 16 - Grey and Gatehouse, 1978, 17 - Ercit and Hawthorne, 1995.

and members of the osumilite and nordite groups. These are densely-packed, OH- and H_2O-free structures with edge- and face-sharing polyhedra; substitution of Mn and Fe^{2+} for Zn is limited. The presence or absence of minerals such as those of the osumilite and nordite groups is an excellent indicator of $f_{S^{2-}}$ at these early stages. As crystallization of the alkaline pegmatite continues, temperature and $f_{S^{2-}}$ drop, the magma becomes further saturated with H_2O, and alkalinity and oxidizing potential increase. Zinc, a Lewis base, is highly soluble in these H_2O- and alkali-rich magmas and fluids, and acts as a network modifier, forming $Zn(OH)_4^{2-}$ complexes in the melt (Greenwood and Earnshaw, 1984; Wedepohl, 1969). In addition, the increase in $f_{O^{2-}}$ results in dissolution of early sphalerite, remobilization of Zn, further increasing the concentration of Zn in late-stage magmatic or hydrothermal alkali fluids. Evidence for sphalerite dissolution and Zn remobilization can be observed in the pegmatites of Lovozero, Khibiny and Mont Saint-Hilaire where tetrahedral cavities after dissolved sphalerite, sometimes with sauconite incrustations, hemimorphite or smithsonite, are common. In each large pegmatite, up to several tons of Zn can be remobilized by such late-stage, alkali fluids.

Late-stage magmatic and hydrothermal alkaline pegmatite Zn species are OH- and H_2O-rich, often with open, zeolite- (gaultite, kukisvumite, hemimorphite, labuntsovite-group minerals) or clay-like structures (sauconite, zincsilite, fraiponite). In such $^{[6]}$Zn silicate species, the Zn shows a preference for sites which have two or more OH^- or H_2O molecules as ligands. Although it is not entirely clear why this is the case, it is possible that the high polarizability of Zn, its preference for [4]-coordinated sites, and the lower polarizability of OH^- *vs*. O^{2-} result in a psuedo-[4]-coordinated environment with Zn valence being distributed mainly over the O^{2-} ligands.

Late-stage minerals with $^{[4]}$Zn (gaultite, kukisvumite/manganokukisvumite) show limited Zn $\rightleftharpoons$ (Mn,Fe^{2+}) substitution, whereas those with $^{[6]}$Zn show extensive Zn $\rightleftharpoons$ (Mn,Fe^{2+}) substitution; occupation of [4]-coordinated sites by Fe^{2+} or Mn is facilitated by high temperatures. In gaultite, $Na_4[Zn_2Si_7O_{18}]\cdot 5H_2O$, a true zeolite-group mineral, $^{[4]}$Zn proxies for Al in the framework (Ercit and Van Velthuisen, 1994). The isostructural pair kukisvumite–manganokukisvumite is an excellent example which demonstrates the lack of Zn $\rightleftharpoons$ Mn isomorphism in tetrahedral sites of late hydrous zeolite-like silicates. Gault *et al*. (2004) described from the Kukisvumitovoye pegmatite, (Kukisvumchorr Mine, Khibiny massif, Russia), epitactic intergrowths of concentrically-zoned crystals consisting of almost end-member kukisvumite (0.15 a.p.f.u. Mn) and manganokukisvumite (Zn-free). Similarly, Pekov and Podlesnyi (2004) described new finds of manganokukisvumite with 4.96 wt.% MnO and Zn below detection limit, and kukisvumite with 6.19 wt.% ZnO and 0.52 wt.% MnO, in two other pegmatites at the same Kukisvumchorr Mine. The presence of almost end-member kukisvumite and manganokukisvumite within the same chemically-zoned crystal demonstrates the strong tendency for ordering and partitioning of Mn and Zn in [4]-coordinated sites.

In contrast, in the zeolite-like structures of the labuntsovite-group minerals with [6]-coordinated Zn (organovaite-Zn, kuzmenkoite-Zn, alsakharovite-Zn and lepkhenelmite-Zn), isolated $(Zn,Mn)(O,H_2O)_6$ octahedra link chains of $(Ti,Nb)O_6$ to the $[Si_4O_{12}]^{8-}$ ring framework. A similar situation exists in Zn-rich kupletskite, where sheets of $(Mn,Zn)(O,OH)_6$ octahedra which display extensive Zn $\rightleftharpoons$ Mn isomorphism, are sandwiched between heterogeneous sheets consisting of $[Si_4O_{12}]^{8-}$ cross-linked by $(Ti,Nb)\phi_6$ octahedra. At Mont Saint-Hilaire, Zn-rich kupletskite and Zn-rich niobokupletskite are often associated with wurtzite, the low-f_{S_2} ZnS polymorph, whereas Zn-free species are associated with sphalerite, the high-f_{S_2} ZnS polymorph (Scott and Barnes, 1972; Piilonen *et al*., 2000), suggesting that incorporation of Zn into the AGM structure is a function of f_{S_2} and not a function of temperature as both polymorphs are stable over a wide range of temperatures (Scott and Barnes, 1972). The presence or absence of Zn silicate in an alkaline environment is a complex indicator of f_{S_2}, f_{O_2} and alkalinity. Not only the mineralogy, but also the crystal chemistry of Zn in alkaline systems changes through the evolution of the complex, thus permitting us a unique glimpse into a full range of behaviour of this element.

Acknowledgements

The authors thank Dr Tonci Balić-Žunić of the University of Copenhagen (Denmark) for use of the diffractometer, and Dr Nelson Eby for providing unpublished data from his research on alkaline complexes. Funding for this project was in the form of a RAC grant to PCP (CMN).

Reviews by Dr M. Welch and an anonymous reviewer are greatly appreciated.

References

Agakhanov, A.A., Pautov, L.A., Sokolova, E.V., Hawthorne, F.C. and Belakovskiy, D.I. (2003) Telyushenkoite, $CsNa_6[Be_2Al_3Si_{15}O_{39}F_2]$ – a new cesium mineral of the leifite group. *New Data on Minerals*, **38**, 5–8.

Anderson, T. and Sørensen, H. (1993) Crystallization and metasomatism of nepheline syenite xenoliths in quartz-bearing intrusive rocks in the Permian Oslo rift, SE Norway. *Norsk Geologisk Tidsskrift*, **73**, 250–266.

Bailey, J.C., Gwozdz, R., Rose-Hansen, J. and Sørensen, H. (2001) Geochemical overview of the Ilimaussaq complex, South Greenland. *Geological Survey of Denmark and Greenland Bulletin.*

Brese, N.E. and O'Keefe, M. (1991) Bond-valence parameters for solids. *Acta Crystallographica*, **B47**, 192–197.

Brooks, C.K., Engell, J., Larsen, L.M. and Pedersen, A.K. (1982) Mineralogy of Werner Bjerge alkaline complex, East Greenland. *Meddelelser om Grønland, Geoscience*, **7**, 38 pp.

Christiansen, C.C., Johnsen, O. and Ståhl, K. (1998) Crystal structure of kupletskite from the Kangerdlugssuaq intrusion, East Greenland. *Neues Jahrbuch für Mineralogie Monatshefte,* **6**, 253–264.

Chukanov, N.V., Pekov, I.V., Zadov, A.E., Azarova, Yu.V. and Semenov, E.I. (2002) Kuzmenkoite-Zn, $K_2Zn(Ti,Nb)_4(Si_4O_{12})_2(OH,O)_4{\cdot}6\text{-}8H_2O$, a new labuntsovite-group mineral from the Lovozero massif, Kola peninsula. *Zapiski Vserossiyskogo Mineralogicheskogo Obshchestva*, **131**, 2, 45–50.

Chukhrov, F.V. (editor) (1972) *Minerals Reference Book*, Vol. III, 1. Nauka Publishing, Moscow (in Russian).

Cromer, D.T. and Liberman, D. (1970) Relativistic calculation of anomalous scattering factors for X-rays. *Journal of Chemical Physics*, **53**, 1891–1898.

DeMark, R.S. (1984) Minerals of Point of Rocks, New Mexico. *Mineralogical Record*, **15**, 149–156.

Eby, G.N. (2004) Petrology, geochronology, mineralogy and geochemistry of the Beemerville alkaline complex, northern New Jersey. Pp. 52–68 in: *Neoproterozoic, Paleozoic and Mesozoic Intrusive Rocks of Northern New Jersey and Southeastern New York* (J.H. Puffer and R.A. Volkert, editors). 21st Annual Meeting, Geological Association of New Jersey, Mahwah, NJ.

Eby, G.N., Woolley, A.R., Din, V. and Platt, G. (1998) Geochemistry and petrogenesis of nepheline syenites: Kasungu-Chipala, Ilomba, and Ulindi nepheline syenite intrusions, North Nyasa Alkaline Province, Malawi. *Journal of Petrology*, **39**, 1405–1424.

Ercit, T.S. and Hawthorne, F.C. (1995) Murataite, a UB12 derivative structure with condensed Keggin molecules. *The Canadian Mineralogist*, **33**, 1223–1229.

Ercit, T.S. and van Velthuisen, J. (1994) Gaultite, a new zeolite-like mineral species from Mont Saint-Hilaire, Quebec, and its crystal structure. *The Canadian Mineralogist*, **32**, 855–863.

Faure, G. (1991) *Principles and Applications of Inorganic Geochemistry*. MacMillian Publishing Company, New York.

Ferraris, G., Prencipe, M., Pautov, L.A. and Sokolova, E.V. (1999) The crystal structure of darapiosite and a comparison with Li- and Zn-bearing minerals of the milarite group. *The Canadian Mineralogist*, **37**, 769–774.

Flohr, M.J.K. and Ross, M. (1990) Alkaline igneous rocks of Magnet Cove, Arkansas: Mineralogy and geochemistry of syenites. *Lithos*, **26**, 67–98.

Gault, R.A., Ercit, T.S., Grice, J.D. and Van Velthuizen, J. (2004) Manganokukisvumite: a new mineral species from Mont Saint-Hilaire, Quebec. *The Canadian Mineralogist*, **42**, 781–785.

Ghose, S. (1964) The crystal structure of hydrozincite, $Zn_6(OH)_6(CO_3)_2$. *Acta Crystallographica*, **17**, 1051–1057.

Greenwood, N.N. and Earnshaw, A. (1984) *Chemistry of the Elements*. Pergamon Press, Oxford, UK, pp. 1395–1422.

Grey, I.E. and Gatehouse, B.M. (1978) The crystal structure of landauite, $Na[MnZn_2(Ti,Fe)_6Ti_{12}]O_{38}$. *The Canadian Mineralogist*, **16**, 63–68.

Hassan, I. and Grundy, H.D. (1985) The crystal structures of helvite group minerals, $(Mn,Fe,Zn)_8(Be_6Si_6O_{24})S_2$. *American Mineralogist*, **70**, 186–192.

Horváth, L. and Gault, R.A. (1990) The mineralogy of Mont Saint-Hilaire, Québec. *Mineralogical Record*, **21**, 284–359.

Kadar, M. (1984) *Mineralogie et implications petrologiques des pegmatites des syenites nepheliniques du massif alcalin du Tamazeght (Haut Atlas de Midelt, Maroc)*. These 3eme cycle, Université Paul Sabatier, Toulouse, France.

Kostyleva-Labuntsova, E.E., Borutskii, B.E., Sokolova, M.N., Shlyukova, Z.V., Dorfman, M.D., Dudkin, O.B. and Kozyreva, L.V. (1978) *Mineralogy of the Khibiny Massif*. Vol. 2. Nauka Publishing, Moscow (in Russian).

Kovalenko, V.I. (1977) The geochemical trend in the evolution of alkali granite magmas. *Geochemica International*, **6**, 41–53.

Liebau, F. (1985) *Structural Chemistry of Silicates: Structure, Bonding and Classification*. Springer-

Verlag, Berlin.

Markl, G. (2001) A new type of silicate liquid immiscibility in peralkaline nepheline syenites (lujavrites) of the Ilimaussaq complex, South Greenland. *Contributions to Mineralogy and Petrology*, **141**, 458–472.

McDonald, W.S. and Cruickshank, D.W.J. (1967) Refinement of the structure of hemimorphite. *Zeitschrift für Kristallographie, Kristallgeometrie, Kristallphysik, Kristallchemie.* **124**, 180–191.

Merlino, S., Pasero, M. and Ferro, O. (2000) The crystal structure of kukisvumite, $Na_6ZnTi_4(Si_2O_6)_4O_4{\cdot}4(H_2O)$. *Zeitschrift für Kristallographie*, **215**, 352–356.

Pekov, I.V. (2002) New zincian minerals and genetic aspect of the crystal chemistry of zinc in hyperalkaline pegmatites. Abstract. *New Approach to the Study and Description of Minerals and Mineral Formation Processes*. Moscow, pp. 35–37.

Pekov, I.V. (2005) *Genetic Mineralogy and Crystal Chemistry of Rare Elements in High-Alkaline Postmagmatic Systems*. D.Sc. thesis, Moscow State University.

Pekov, I.V. and Podlesnyi, A.S. (2004) Kukisvumchorr Deposit: Mineralogy of Alkaline Pegmatites and Hydrothermalites. *Mineralogical Almanac*, **7**, 1–164.

Pekov, I.V., Chukanov, N.V., Kononkova, N.N., Belakovskiy, D.I., Pushcharovsky, D.Yu. and Vinogradova, S.A. (1998) Ferronordite-(Na), $Na_3SrCeFeSi_6O_{17}$, and manganonordite-(Na), $Na_3SrCeMnSi_6O_{17}$, new minerals from Lovozero massif, Kola peninsula. *Zapiski Vserossiyskogo Mineralogicheskogo Obshchestva*, **127**, 48–57.

Pekov, I.V., Chukanov, N.V., Turchkova, A.G. and Grishin, V.G. (2001) Ferronordite-(La), $Na_3Sr(La,Ce)FeSi_6O_{17}$ – a new mineral of the nordite group from Lovozero massif, Kola Peninsula. *Zapiski Vserossiyskogo Mineralogicheskogo Obshchestva*, **130**, 53–58.

Pekov, I.V., Chukanov, N.V., Zadov, A.E., Krivovichev, S.V., Azarova, Yu.V., Burns, P.C. and Schneider, J. (2002) Organovaite-Zn, $K_2Zn(Nb,Ti)_4(Si_4O_{12})_2(O,OH)_4{\cdot}6H_2O$, a new mineral of the labuntsovite group. *Zapiski Vserossiyskogo Mineralogicheskogo Obshchestva*, **131**, 29–34.

Pekov, I.V., Chukanov, N.V., Zadov, A.E., Rozenberg, K.A. and Rastsvetaeva, R.K. (2003) Alsakharovite-Zn, $NaSrKZn(Ti,Nb)_4[Si_4O_{12}]_2(O,OH)_4{\cdot}7H_2O$, a new mineral of the labuntsovite group from Lovozero massif, Kola Peninsula. *Zapiski Vserossiyskogo Mineralogicheskogo Obshchestva*, **132**, 52–58.

Pekov, I.V., Chukanov N.V., Shilov, G.V., Kononkova, N.N. and Zadov, A.E. (2004) Lepkhenelmite-Zn, $Ba_2Zn(Ti,Nb)_4[Si_4O_{12}]_2(O,OH)_4{\cdot}7H_2O$, a new mineral of the labuntsovite group and its crystal structure. *Zapiski Vserossiyskogo Mineralogicheskogo Obshchestva*, **133**, 49–58.

Piilonen, P.C., Lalonde, A.E., McDonald, A.M. and Gault, R.A. (2000) Niobokupletskite, a new astrophyllite-group mineral from Mont Saint-Hilaire, Québec, Canada: Description and crystal structure. *The Canadian Mineralogist*, **38**, 627–639.

Piilonen, P.C., McDonald, A.M. and Lalonde, A.E. (2001) Kupletskite polytypes from the Lovozero massif, Kola Peninsula, Russia: Kupletskite-1A and kupletskite-*Ma2b2c*. *European Journal of Mineralogy*, **13**, 973–984.

Piilonen, P.C., Lalonde, A.E., McDonald, A.M., Gault, R.A. and Larsen, A.O. (2003*a*) Insights into astrophyllite group minerals I: Nomenclature, composition and development of a standardized general formula. *The Canadian Mineralogist*, **42**, 1–26.

Piilonen, P.C., McDonald, A.M. and Lalonde, A.E. (2003*b*) Insights into the astrophyllite group II: Crystal chemistry. *The Canadian Mineralogist*, **42**, 27–54.

Raade, G. and Haug, J. (1982) Gjerdingen-Fundstelle seltener Mineralien in Norwegen. *Lapis*, **7**, 9–15.

Rule, A.C. and Radke, F. (1988) Baileychlore, the Zn end member of the trioctahedral chlorite series. *American Mineralogist*, **73**, 135–139.

Scott, S.D. and Barnes, H.L. (1972) Sphalerite-wurtzite equilibria and stoichiometry. *Geochimica et Cosmochimica Acta*, **36**, 1275–1295.

Semenov, E.I. (1956) Kupletskite – a new mineral of the astrophyllite group. *Doklady Akademii Nauk SSSR*, **108**, 933–936.

Sheldrick, G.M. (1993) *SHELXL-93*. Program for the refinement of crystal structures. University of Göttingen, Germany.

Shi, N., Ma, Z., Li, G., Yamnova, N.A. and Pushcharovsky, D.Y. (1998) Structure refinement of monoclinic astrophyllite. *Acta Crystallographica*, **B54**, 109–114.

Sokolova, E.V., Rybakov, V.B. and Pautov, L.A (1999) Crystal structure of shibkovite. *Doklady Akadamii Nauk*, **369**, 378–380.

Sveshnikova, E.V., Semenov, E.I. and Khomyakov, A.P. (1976) *Zaangarskii Alkaline Massif, its Rocks and Minerals*. Nauka Publishing, Moscow (in Russian).

Valter, A.A., Eryomenko, G.K. and Leesenko, T.A. (1965) Kupletskite from the alkaline rocks of the Azov Region. *Russian Physics Journal*, **19**, 248–252.

Wedepohl, K.H. (1969) *Handbook of Geochemistry I*. Springer-Verlag, Berlin, 30A–30O.

Woolley, A.R. and Platt, G.R. (1988) The peralkaline nepheline syenites of the Junguni intrusion, Chilwa province, Malawi. *Mineralogical Magazine*, **52**, 425–433.

[*Manuscript received 8 March 2006: revised 5 October 2006*]